

# Pattern Formation of Ion Channels with State Dependent Electrophoretic Charges and Diffusion Constants in Fluid Membranes

S. C. Kramer and R. Kree

*Institut für Theoretische Physik, Georg-August-Universität Göttingen, Bunsenstr. 9, 37073 Göttingen*

A model of mobile, charged ion channels in a fluid membrane is studied. The channels may switch between an open and a closed state according to a simple two-state kinetics with constant rates. The effective electrophoretic charge and the diffusion constant of the channels may be different in the closed and in the open state. The system is modeled by densities of channel species, obeying simple equations of electro-diffusion. The lateral transmembrane voltage profile is determined from a cable-type equation. Bifurcations from the homogeneous, stationary state appear as hard-mode, soft-mode or hard-mode oscillatory transitions within physiologically reasonable ranges of model parameters. We study the dynamics beyond linear stability analysis and derive non-linear evolution equations near the transitions to stationary patterns.

## I. INTRODUCTION

Spontaneous pattern formation of ion channels in cell membranes has been a subject of continuous interest during recent years [1–3]. Spatially modulated distributions of ion channels or pumps are ubiquitous in many cells. They are closely related to important biological functions like some early stages of morphogenesis [4] or the storage and processing of information in neural tissue [5]. Many physiological regulation processes involve changes of ion fluxes through cell membranes on time scales ranging from milliseconds to hours [6].

There have been attempts to explain the aggregation of channel proteins in a fluid membrane on the basis of thermodynamic models [1], [7] and references therein. Typically the system of channels is driven out of equilibrium due to ionic concentration gradients and transmembrane fluxes. Therefore, a number of authors have put forward models for spontaneous pattern formation based upon systems of semi-phenomenological, non-equilibrium equations of motion for the densities of channel proteins, the charge densities of ions and the intra- and extracellular voltage [1,3,8]. In many important systems like axons or cells in neural or muscular tissue, there is a bulk volume of aqueous solution of ions on one side of the membrane whereas on the other side, there is only a thin layer of electrolyte, whose thickness usually is in the range of  $10 \dots 100$  nm. See Fig.1 For a schematic picture of the situation. Under these conditions, the models may be simplified further. Ion densities may be eliminated approximately, leading to a coupling of the densities of channels to the lateral transmembrane voltage profile within that layer. The voltage profile has to be determined from a quasi one-dimensional or two-dimensional cable equation [2,9,10]. This contains transmembrane currents and thus channels are effectively coupled via the transmembrane voltage.

In the present work we will follow this approach and analyze a model of charged ion channels, which may switch between a closed and an open state, thereby also changing their effective electrophoretic charge and their diffusion constant. The effective electrophoretic charge can be of both signs - although the proteins are usually only negatively charged - if the electro-osmotic effect is taken into account [8].

We consider this model as a natural, minimal model of mobile channels with kinetics of internal states. As the conformations, which change the states of an ion channel [11,12], may involve charge transport across the membrane [12,13] as well as binding to other molecules, for instance phosphorylation via protein kinase or immobilization due to binding to the cytoskeleton [13,14], the state dependence of charge and diffusion constant should be taken into account.

In [2] a special case of the present model has been studied already. The authors of this work considered a reservoir of closed channels in the well-stirred approximation without coupling to the lateral voltage profile. We will see below that our model leads to qualitatively different behavior in a wide range of parameters but still contains the results of [2]. The necessary limit is that closed channels diffuse faster than the open ones and that their electrophoretic charge vanishes. The present model is also related to [15], where a mixture of two different channels has been considered without a kinetic, which allows for transitions between the different species.

The basic mechanism, which drives spontaneous pattern formation is very simple in models, which only involve mobile, charged ion channels and the lateral profile of the transmembrane voltage [3]. It is based on a feedback loop during which the channel proteins drift due to lateral voltage gradients and at the same time modify the voltage gradients by Ohmic voltage drops, caused by transmembrane currents. Therefore, for example, neg-

actively charged channels, which cause currents directed into the thin layer of electrolyte have a tendency to aggregate. Diffusion will counteract this tendency and thence a variety of bifurcations of the homogeneous state to an inhomogeneous state becomes possible. We will show below that our model implies a number of different scenarios for the first bifurcation from the homogeneous state.

Depending on parameter ranges either soft-mode instabilities arise, where periodic patterns appear with a wavenumber  $k_c$ , which approaches zero at the transition. Or there will be different kinds of hard-mode instabilities, where patterns with  $k_c \neq 0$  at the transition and spatio-temporal patterns emerge with non-vanishing  $k_c$  and non-vanishing frequency  $\Omega_c$ .

After introducing the model in the next section, we will give results of the linear stability analysis together with results of non-linear behavior close to transitions into stationary patterns in subsequent sections. For soft-mode instabilities, we derive a Cahn-Hilliard type equation of motion for the slow modes near the transition. For hard-mode instabilities, an amplitude equation is derived, which allows us to separate parameter regions of forward and backward bifurcation or continuous and discontinuous transitions respectively.

## II. THE MODEL

We consider ion channels moving within a fluid membrane of size  $L_x \times L_y$  which separates a thin layer of electrolyte of width  $d$  from an electrolytic bath, as it is sketched in Fig.1. Positions  $\mathbf{r}$  within the membrane are described by internal rectilinear coordinates  $\mathbf{r} = (x, y)$ ,  $0 \leq x < L_x$ ,  $0 \leq y < L_y$ . If we choose periodic boundary conditions in the  $y$  coordinate, the membrane corresponds to a cylindrical cable and is reminiscent of axonic or dendritic structures for  $L_x \gg L_y$ . Note that we treat  $L_y$  and  $d$  as independent quantities, so that the actual structure in cylindrical geometry looks like on the right hand side of Fig.1, with a sub-membrane layer of width  $d$  and a 'core' of radius  $(L_y/2\pi) - d$ , which is decoupled from the sub-membrane layer. For  $d = L_y/2\pi$  the sub-membrane layer fills the entire interior of the cable. In the following we will not distinguish between these different geometries, as the present work only deals with infinitely extended systems and hence effects of specific boundary conditions need not be taken into account.

Ion channels may switch between an open state (' $o$ ') and a closed state (' $c$ ') according to a simple monomolecular chemical reaction scheme



with rates  $\gamma_-$  and  $\gamma_+$ . We are interested in a wide range of kinetic rates, from  $10^3$ /sec for voltage or ligand gated channels down to less than one per hour as it is observed

for hormone regulated phosphorylation and dephosphorylation of channel proteins. The distribution of channels is described by smooth densities  $n_r(\mathbf{r}, t)$ ,  $r \in \{o, c\}$ , which obey the equations

$$\partial_t n_r(\mathbf{r}, t) + \nabla \mathbf{j}_r(\mathbf{r}, t) = \sigma_r [\gamma_+ n_c(\mathbf{r}, t) - \gamma_- n_o(\mathbf{r}, t)] \quad (2)$$

with  $\sigma_r = +1$  for  $r = o$  and  $\sigma_r = -1$  for  $r = c$ . The *rhs* of this equation takes into account the reaction kinetics of (1). Current densities  $\mathbf{j}_r$  of the channels are assumed to be of the Nernst-Planck form

$$\mathbf{j}_r(\mathbf{r}, t) = -D_r \{ \nabla n_r(\mathbf{r}, t) - \beta n_r(\mathbf{r}, t) \cdot q_r \mathbf{E}(\mathbf{r}, t) \} \quad (3)$$

where  $D_r$  and  $q_r$  refer to the constants of lateral diffusion and to the effective electrophoretic charges of open and closed channels, respectively. The coefficient  $\beta$  is the inverse temperature and  $\mathbf{E}(\mathbf{r}) = -\nabla V(\mathbf{r})$  denotes the lateral electric field. Note that we explicitly allow for different diffusion constants and different electrophoretic charges in the states  $o$  and  $c$ . The simple form of the current densities given in (3) may be justified for rigid protein structures with charged protuberances extending in the intra- and extracellular electrolyte. As discussed in [8], the effective electrophoretic charges may be of both signs due to electro-osmotic effects, although proteins are usually negatively charged.

As has been discussed in the literature [10], the Kelvin cable equation or its two dimensional analogue may be used to calculate the lateral variations of the transmembrane potential provided that spatial variations of ion concentrations have negligible effects and that the characteristic length scales of lateral patterns are large compared to the width of the thin layer of electrolyte. In [10], the cable equation is derived by integrating the Nernst-Planck equation of ion densities together with the Poisson equation using appropriate boundary conditions at the membrane. In the following we use the 2-dimensional cable equation [2]

$$C_m \partial_t V(\mathbf{r}, t) = \frac{d}{\rho_e} \nabla^2 V(\mathbf{r}, t) - G V(\mathbf{r}, t) - \lambda n_o(\mathbf{r}, t) \{ V(\mathbf{r}, t) - E \}. \quad (4)$$

$C_m$  denotes membrane capacitance per area,  $\rho_e$  the resistivity of the electrolyte within the thin layer of width  $d$ , and  $\lambda n_o$  is the conductance of open channels. We have included a passive, homogeneously distributed transmembrane conductance  $G$ .  $E$  is the reversal potential of ion fluxes through the open channels, which drives the system out of equilibrium.

We are interested in the stability of the homogeneous and stationary solution  $\bar{V}, \bar{n}_o, \bar{n}_c$  of (4)

$$\bar{V} = \frac{\lambda \bar{n}_o E}{G + \lambda \bar{n}_o}, \quad (5)$$

$$\bar{n}_o = \frac{\gamma_+}{\Gamma} \bar{n}, \quad \bar{n}_c = \frac{\gamma_-}{\Gamma} \bar{n}.$$

We consider the total density of channels  $\bar{n}$  as constant and define  $\Gamma := \gamma_+ + \gamma_-$ . Furthermore, we introduce appropriately normalized deviations from the stationary and homogeneous solution as the new fields  $\rho = (n_o - \bar{n}_o)/\bar{n}_o$ ,  $\zeta = (n_c - \bar{n}_c)/\bar{n}_c$  for the open and closed channels, respectively, and  $\Phi = \beta q_o(V - \bar{V})/\bar{V}$  for the membrane potential. Next, we change to dimensionless lengths and times by using as units the typical decay length  $\ell_V = [(\rho_e/d)(\lambda\bar{n}_o + G)]^{-1/2}$  of  $V$  and a typical diffusion time  $\tau = \ell_V^2/D_o$  over this length. Then (2), (3) and (4) become dimensionless

$$\partial_t \varrho = \nabla \{ \nabla \varrho + (\varrho + 1) \nabla \Phi \} - \gamma_- (\varrho - \zeta), \quad (6)$$

$$\partial_t \zeta = D \nabla \{ \nabla \zeta + q(\zeta + 1) \nabla \Phi \} + \gamma_+ (\varrho - \zeta), \quad (7)$$

$$\epsilon \partial_t \Phi = [\nabla^2 - 1] \Phi - \alpha \Phi \varrho - \eta \varrho. \quad (8)$$

In these equations we use the ratio of diffusion constants  $D = D_c/D_o$ , of electrophoretic charges  $q = q_c/q_o$ , the relative conductivity of the membrane  $\alpha = \lambda\bar{n}_o/(\lambda\bar{n}_o + G)$  and a rescaled reversal potential  $\eta = -\alpha(1 - \alpha)\beta q_o E$ . The parameter  $\epsilon = C_m \rho_e D_o/d$  compares the electrical relaxation (RC) time per area to the diffusion constant. Note that  $\gamma_+$  and  $\gamma_-$  have also been made dimensionless  $\gamma_{\pm} \rightarrow \gamma_{\pm} \tau$  by multiplication with  $\tau$ .

For cell membranes, the parameters in (2), (3) and (4) imply time-scales, which differ by several orders of magnitude. Typical parameter values are [12]  $C_m = 1 \mu\text{F}/\text{m}^2$ ,  $\rho_e \sim 1 \Omega\text{m}$ ,  $d \sim 10\text{nm}$ , and  $D_r \sim 0.1(\mu\text{m})^2/\text{sec}$  for diffusion of mobile proteins. Channel conductances  $\lambda$  are in the  $10^{-12}\Omega^{-1}$  range, average channel densities are around  $10 \cdot \dots \cdot 50 (\mu\text{m})^{-2}$  and electrotonic lengths  $\ell_V$  are of the order of a few  $\mu\text{m}$ . Then the unit  $\tau \sim 10^2\text{sec}$ , whereas the electrical relaxation time is below  $1\mu\text{sec}$  and it is always the smallest time scale of the system, even compared to fast kinetics of voltage or ligand gated channels with time constants in the msec range. The constant  $\epsilon \sim 10^{-7}$ . This separation of time scales justifies the use of the quasi-stationary approximation in (8) and hence we will put the *rhs* of (8) equal to zero in the following. For voltage or ligand gated channels, the time-scale set by the rate  $\Gamma$  is also very fast compared to  $\tau$ ,  $\Gamma \sim 10^5$ , whereas slower regulation processes have time-scales comparable to or larger than  $\tau$ . The limit  $\Gamma \gg 1$  will be referred to as *fast reaction limit* in the following.

For reversal potentials  $|E| \sim 0 \dots 100\text{mV}$  and electrophoretic charges of a few elementary units the parameter  $\eta$  is in the range  $|\eta| \sim 0 \dots 10$  under physiological conditions.

### III. LINEAR STABILITY ANALYSIS

We linearize (6-8) around the homogeneous and stationary solution (5) and apply the plane wave Ansatz  $(\varrho, \zeta, \Phi) = (\varrho_k, \zeta_k, \Phi_k) \exp\{i\mathbf{k} \cdot \mathbf{x} + \omega t\} + c.c.$

As it was discussed above, within the quasi-stationary approximation potential fluctuations  $\Phi_k$  are proportional to fluctuations of open channels

$$\Phi_k = -\eta \varrho_k / (1 + k^2). \quad (9)$$

Inserting (9) into the linearized (6) and (7) we get by abbreviating  $\eta_k = \eta/(1 + k^2)$  the eigenvalue problem

$$\omega \begin{pmatrix} \varrho_k \\ \zeta_k \end{pmatrix} = \left\{ \begin{pmatrix} -\gamma_- & \gamma_- \\ \gamma_+ & -\gamma_+ \end{pmatrix} - k^2 \begin{pmatrix} 1 - \eta_k & 0 \\ -Dq\eta_k & -D \end{pmatrix} \right\} \begin{pmatrix} \varrho_k \\ \zeta_k \end{pmatrix}. \quad (10)$$

The eigenvalues

$$\omega_{\pm} = -[P(k^2) \pm \sqrt{Q(k^2)}]/2$$

$$P(k^2) = k^2(1 + D - \eta_k) + \Gamma$$

$$Q(k^2) = [k^2(1 - D - \eta_k) + \gamma_- - \gamma_+]^2 + 4Dq\gamma_- \eta_k + 4\gamma_- \gamma_+ \quad (11)$$

determine linear stability. Let us note in passing that an extended model with voltage dependent reaction rates will lead to the same set of linearized equations.

The solution (5) becomes unstable against small perturbations if  $\text{Re} \omega_+$  or  $\text{Re} \omega_-$  is positive. Note that oscillatory unstable modes, which require  $\text{Im} \omega_{\pm} \neq 0$  and thus  $Q < 0$ , are possible in the parameter range  $q\eta < 0$ .

The decisive influence of the parameters  $\eta$  and  $q$  on the qualitative behavior of solutions is already apparent in the fully non-linear system (6-8). The term  $\eta \varrho$  in (8) drives the curvature of the potential  $\Phi$ , whereas  $q$  may change the relative direction of drift currents of the closed channels. For example, if open channels carry negative charge, their drift is directed towards depolarized regions of the membrane, where they accumulate. If a current through open channels is directed into the thin layer of electrolyte, this current will further depolarize the membrane and may cause an instability. If closed channels have a positive effective electrophoretic charge, the accumulated open channels will disperse again after closing. This may lead to an oscillatory behavior. By varying the relative signs of  $q$  and  $\eta$ , different scenarios of aggregation and dispersion of channels by lateral structures in  $\Phi$  may arise, which are coupled back into the (8) and may lead to stationary or oscillatory patterns.

In the following we will hence discuss the four parameter regions  $\mathcal{R}_{++} \hat{=} \{q > 0, \eta > 0\}$ ,  $\mathcal{R}_{--} \hat{=} \{q < 0, \eta < 0\}$ ,  $\mathcal{R}_{+-} \hat{=} \{q > 0, \eta < 0\}$  and  $\mathcal{R}_{-+} \hat{=} \{q < 0, \eta > 0\}$  separately. The quantity  $\eta$  is treated as the primary control parameter.

## A. Instabilities for $q\eta > 0$

In these regions of parameters,  $Q(k^2)$  is always positive, the rates  $\omega_{\pm}(k^2)$  are real and thus plane wave solutions will either exponentially grow or decay in time. Instabilities signal the onset of stationary patterns. As  $\omega_+ > \omega_-$ , it is the rate  $\omega_+$ , which will drive the solution (5) unstable, if control parameters reach the stability boundary. Note that in the long wavelength limit  $k \rightarrow 0$ ,  $\omega_+$  vanishes for all values of  $\eta, q, D, \gamma_{\pm}$  like  $\omega_+ = O(k^2)$ . The corresponding diffusion mode reflects conservation of the total number of channels.

From  $\omega_+\omega_- = 0$  we get the neutrality condition

$$\eta_0(k) = (1 + k^2) \frac{D(k^2 + \gamma_-) + \gamma_+}{D(k^2 + q\gamma_-) + \gamma_+}. \quad (12)$$

The minimum of  $\eta_0(k)$  corresponds to the first onset of instabilities and the corresponding wavenumber  $k_c$  is the first unstable mode (critical mode). A minimum of the neutral curve appears at  $k_c \neq 0$  with

$$k_c^2 = -q\gamma_- - \frac{\gamma_+}{D} + \sqrt{\gamma_-(q-1)(q\gamma_- + \gamma_+/D - 1)} \quad (13)$$

if the *rhs* of (13) is a positive, real number. By varying  $q, D$  or the rates  $\gamma_{\pm}$ , the instability may switch between soft-mode ( $k_c = 0$ ) and hard-mode ( $k_c \neq 0$ ) type.

Several statements are noticeable: (a) For  $D = 0$ , (immobile closed channels), as well as for  $q = 1$ , the neutrality condition,  $\eta_0 = 1 + k^2$ , is independent of the reaction rates and implies a soft mode instability at  $\eta_c = 1$ . A hard mode instability requires both mobile channels and different charges of closed and open states. (b) Hard mode instabilities are only possible for  $q < 1$ , i.e.  $q_c < q_o$ . (c) For  $D \rightarrow \infty$  and  $q = 0$  we recover the result of [2]. (d) In the fast reaction limit ( $\gamma_- \gg 1, \gamma_+ \gg 1, D \neq 0$ ), only soft mode instabilities at  $\eta_c = (D\gamma_-/\gamma_+ + 1)/(Dq\gamma_-/\gamma_+ + 1)$  remain. Note that the critical control parameter stays small ( $O(1)$ ) in the fast reaction limit, indicating that the instability may indeed be reached under physiological conditions.

For reaction rates of order 1, typical curves of  $\eta_0(k)$  are shown in Fig.2. Whereas in  $\mathcal{R}_{++}$ , both soft and hard mode instabilities may occur, a neutral curve in  $\mathcal{R}_{--}$  does only appear for  $D|q| > \gamma_+/\gamma_-$ , in which case  $\eta_0(k)$  is maximal at  $k = 0$  and exhibits poles at  $k_p^2 = -q\gamma_- - \gamma_+/D$ . Thus, for electrophoretic charges  $q_o$  and  $q_c$  of different signs, merely soft-mode instabilities at  $\eta_c < 0$  are possible as it is demonstrated in Fig.2.b). Note that only a finite band of unstable modes, limited to the interval  $(-k_p, k_p)$ , will appear for all  $\eta < 0$ . This unstable band grows like  $k_p \sim \Gamma^{1/2}$  in the fast reaction limit. Fig.3 shows the  $k_c^2 = 0$  lines in the  $D$ - $\Gamma$ -plane for different values of  $q$ . For parameters  $(D, \Gamma)$  below each curve  $k_c^2 \neq 0$ .

Setting  $q_{k_c} = 1$  and solving the linearized system for the eigenvector  $(\varrho_{k_c}, \zeta_{k_c}, \Phi_{k_c})$  of the critical mode, we obtain  $\zeta_{k_c} = (qk_c^2 + q\gamma_- + \gamma_+/D)/(k_c^2 + q\gamma_- + \gamma_+/D)$  and

$\Phi_{k_c} = -(k_c^2 + q\gamma_- + \gamma_+/D)/(k_c^2 + q\gamma_- + \gamma_+/D)$ . Taking a closer look at the signs we find  $\text{sgn } \varrho_{k_c} = \text{sgn } \zeta_{k_c}$  and  $\text{sgn } \varrho_{k_c} = -\text{sgn } \Phi_{k_c}$  if  $q > 0$ . Hence for  $q > 0$ , spatial variations of open and closed channels are in phase but have a phase lag of  $\pi$  with respect to the potential in the critical mode. But if  $q < 0$  there is no phase lag, as then  $\text{sgn } \varrho_{k_c} = \text{sgn } \zeta_{k_c} = \text{sgn } \Phi_{k_c}$ . In this case the critical wavenumber vanishes leading to  $\zeta_0 = 1$  and  $\Phi_0 = -\eta_c$  so that all spatial periods are in phase as expected from the qualitative discussion on the mechanism of pattern formation given in (II) after (8).

## B. Instabilities for $q\eta < 0$

The simplest behavior of the system appears in the regime  $\mathcal{R}_{+-}$ . For  $\text{Im}\omega_{\pm} \neq 0$ , it is obvious from (11) that  $\text{Re}\omega_{\pm} = -(1/2)P(k^2) < 0$ . It is easy to show that linear stability also holds for  $\text{Im}\omega_{\pm} = 0$  and thus the homogeneous, stationary solution (5) is linearly stable in this regime.

It is only in  $\mathcal{R}_{-+}$ , that oscillatory instabilities may arise, because  $Q(k^2)$  and  $P(k^2)$  can simultaneously take on negative values in this regime. If  $Q < 0$ ,  $\omega_+ = \omega_-^*$ , and the growth rate of the perturbation is  $\text{Re}\omega_{\pm} = -P(k^2)/2$ . From the condition  $P(k^2, \eta) = 0$  we obtain the neutrality condition  $\eta_P(k)$  for oscillatory instabilities

$$\eta_P(k) = (1 + D)(1 + k^2) \left( 1 + \frac{\Gamma}{(1 + D)k^2} \right). \quad (14)$$

It attains its minimum at the critical wavenumber

$$k_{P_c} = 4 \sqrt{\frac{\Gamma}{1 + D}}. \quad (15)$$

The critical value of the control parameter is

$$\eta_{P_c} = (1 + D) \left( 1 + \sqrt{\frac{\Gamma}{1 + D}} \right)^2. \quad (16)$$

Note that  $P(k^2)$  does not depend on the ratio  $q$  of the electrophoretic charges and thus the neutral curve only depends on reaction rates and diffusion coefficients. The ratio  $q$  will, however, show up in the oscillation frequency  $\Omega_c = (1/2)\sqrt{|Q(k_c^2)|}$  at the critical point.

The region  $\mathcal{R}_{-+}$  also contains parts with  $Q(k^2) > 0$ , where stationary unstable patterns may arise if the neutral curve determined from (12) is crossed. Hence the true critical point is located at

$$\eta_c = \min_k \{ \eta_0(k), \eta_P(k) \}. \quad (17)$$

The oscillatory instabilities will not be attainable in the fast reaction limit under physiological conditions because  $\eta_{P_c} \sim \Gamma$  for large  $\Gamma$ .

Fig.4 shows neutral curves in  $\mathcal{R}_{-+}$  together with the region  $Q(k^2) < 0$  for two cases, which differ by the value

of  $D$ . In Fig.4.a, the unstable pattern is oscillating, in Fig.4.b, it is stationary. Fig.5 shows the dependence of the critical frequency  $\Omega_c$  on  $D$  and  $\Gamma$  for different  $q$ . Note, that by decreasing  $D$ , the oscillations will set in with a finite frequency at the transition, whereas by increasing  $D$  the critical frequency  $\Omega_c$  starts out from  $\Omega_c = 0$  at the transition.

#### IV. EFFECTS IN THE WEAKLY NONLINEAR REGIME

We now turn to a discussion of the behavior of the system beyond linear stability analysis. This discussion is restricted to stationary patterns. A more detailed analysis of oscillatory patterns will be given elsewhere.

In the vicinity of the critical control parameter  $\eta_c$  and the critical wavenumber  $k_c$  the linear dispersion of the slow mode  $\omega_+(\eta, k^2)$  may be expanded to obtain the linear part of a non-linear evolution equation for the slow mode near the bifurcation point. From (11) one gets

$$\omega_+(\eta, k^2) = k^{z_a-2} \tau_a^{-1} \left\{ \frac{\eta - \eta_c}{\eta_c} + \xi_a^2 (k - k_c)^2 + O[(k - k_c)^4] \right\}, \quad (18)$$

where  $z_a = 4$  for soft-mode instabilities ( $a = s$ ) and  $z_a = 2$  for hard-mode instabilities ( $a = h$ ). The expressions for time scales  $\tau_a$  and length scales  $\xi_a$  can be found in Appendix A for soft-mode and in Appendix B for hard-mode instabilities.

##### A. Soft-Mode Instabilities

To proceed beyond the linearized dynamics near a soft-mode instability, it is convenient to introduce the variable  $u = (\gamma_+ \varrho + \gamma_- \zeta) / \Gamma$ , which corresponds to fluctuations of the total channel density,  $u = (n_o + n_c - \bar{n}) / \bar{n}$ , and which contains the critical slow mode as  $\eta \rightarrow \eta_c$ . Furthermore we introduce  $v = (\varrho - \zeta) / \Gamma$ , which remains fast relative to  $u$  near the bifurcation. We get an equation for the slowly varying part of  $u(x, t)$  from a gradient expansion, which is outlined in Appendix A.

If we take into account all terms of  $O(\nabla^2)$  and include the  $O(\nabla^4)$  terms, which arise from the linear dispersion (18), the resulting equation for  $u$  takes on the form of a dynamical Cahn-Hilliard ( or 'model B') equation

$$\partial_t u = \tau_s^{-1} \nabla^2 \left\{ \frac{\delta F(u)}{\delta u} \right\} + O(\nabla^4 u^2), \quad (19)$$

with an effective potential  $F(u) = \int [f(u) + (\xi_s^2/2)(\nabla u)^2] d^2 \mathbf{r}$ .

The local part  $f(u)$  is given by

$$f(u) = \frac{\eta_c u^2}{2} + \frac{\eta}{\alpha^2} \left[ (2 - \alpha)u + \left( 1 - \frac{2}{\alpha} - u \right) \ln(1 + \alpha u) \right]. \quad (20)$$

Equation (19) has to be solved under the constraint of conservation of channel number,  $\int u d^2 \mathbf{r} = 0$ , which may be taken into account by an appropriate Lagrange multiplier term  $-\Lambda u$  in  $f(u)$ . Note that the dynamics only depends on the ratio  $\eta_c/\eta$  and on the parameter  $\alpha$  and thus exhibits a particularly simple universality for all permissible values of  $D, q, \gamma_{\pm}$ .

Fig.6 shows the effective potentials for  $\alpha = 0.6$  close to the transition.  $\eta_c$  becomes the spinodal. The discussion of the dynamical behavior, including typical coarsening in the case of quenches can be found in standard textbooks, see for instance [16].

##### B. Hard-Mode Instabilities

In order to obtain an analytic description of the weakly nonlinear regime for hard-mode instabilities, we use a standard multi-scale perturbative approach, which results in an amplitude equation [17]. The approach starts from the Ansatz

$$\mathbf{u}_c [\chi(X, Y, T) e^{ik_c x} + \chi^*(X, Y, T) e^{-ik_c x}] \quad (21)$$

for the fluctuations  $\mathbf{u} = (\varrho, \zeta, \Phi)$ . The amplitude  $\chi$  depends upon the scaled variables  $X = ax$ ,  $Y = a^{1/2}y$  and  $T = a^2 t$ . The scale  $a$  becomes small, if the control parameter  $\eta$  approaches its critical value  $\eta_c$  from above,  $a^2 = (\eta - \eta_c) / \eta_c$ . For convenience we sketch the procedure in Appendix B. For one-dimensional, stationary patterns the perturbation theory gives for the amplitude  $\chi$  in the supercritical vicinity of  $\eta_c$  the equation

$$\tau_h \partial_t \chi = \frac{\eta - \eta_c}{\eta_c} \chi + \xi_h^2 \left[ \partial_x - \frac{i}{2k_c} \partial_y^2 \right]^2 \chi - J |\chi|^2 \chi. \quad (22)$$

The lengthy expression, which gives  $J$  as a function of the model parameters, is given in the Appendix B. Fig.V displays the sign of  $J$  in the  $D$ - $\Gamma$ -plane for different values of  $\alpha$ . Fig.V shows the distribution of the sign of  $J$  within the  $D$ - $\Gamma$ -plane for different values of  $q$  and  $\alpha$ . Positive  $J$  corresponds to a continuous transition (forward bifurcation) negative  $J$  to a discontinuous one (backward bifurcation).

Note that for  $\alpha \leq 0.5$ , Fig.V.a and Fig V.b, there is inside of the domain of  $k_c^2 > 0$  only one region of positive  $J$ , i.e. continuous transitions, which is generically bounded by the domain of negative  $J$ , i.e. discontinuous transitions. In the other regime  $\alpha > 0.5$ , Fig.V.c and Fig V.d, the system shows a reentrant behavior, as then

an additional domain with  $J > 0$  appears below the domain of  $J < 0$ . This means, coming from large values of  $D$  one leaves the area of continuous transitions, crosses the domain of discontinuous transitions and again enters a domain with  $J > 0$ , before finally the  $k_c^2 = 0$ -line is crossed. Parallel to the  $\Gamma$  axis the generic behavior is similar.

## V. CONCLUSIONS

We have studied a simple model of spontaneous pattern formation of mobile ions in a fluid membrane. The channel proteins may switch between an open and a closed state according to a simple two state reaction kinetics with constant rates. The effective electrophoretic charge and the diffusion constant of the channel proteins are assumed to be state dependent. The reversal potential  $E$  of ions, which may pass the open channels constitutes a non-equilibrium driving force. The characterization of a particular model is completed by the additional parameters  $D = D_c/D_o$  and  $q = q_c/q_o$ , the reaction rates  $\gamma_{\pm}$  and the fraction  $\alpha$  of conductance due to the average number of open channels to the average total transmembrane conductivity. Varying these parameters leads to a number of distinct scenarios for first bifurcations from the stationary and homogeneous state. Depending on the sign of the control parameter  $\eta = \alpha(\alpha - 1)\beta q_o E$  and the ratio  $q = q_c/q_o$  of electrophoretic charges, four qualitatively different regions of parameters have been identified from linear stability analysis: (a) for  $q > 0$  and  $\eta > 0$  ( $\mathcal{R}_{++}$ ) soft- or hard mode instabilities leading to stationary patterns will appear, (b) for  $q < 0$  and  $\eta < 0$  ( $\mathcal{R}_{--}$ ) only bifurcations with soft mode instabilities can occur, (c) for  $q < 0$  and  $\eta > 0$  ( $\mathcal{R}_{-+}$ ) hard-mode instabilities with or without temporal oscillations may be found and (d) for  $q > 0$  and  $\eta < 0$  ( $\mathcal{R}_{+-}$ ) the homogeneous, stationary state remains linearly stable. In the fast reaction limit, where the time scale  $\Gamma^{-1}$  becomes much shorter than other time scales (except the RC-relaxation time of transmembrane potential fluctuations), only soft-mode instabilities remain. By varying the ratio  $D = D_c/D_o$  of diffusion constants or  $q = q_c/q_o$  of effective electrophoretic charges within physiologically plausible bounds, it is possible to switch between soft- and hard-mode instability in  $\mathcal{R}_{++}$  and between hard-mode and oscillatory instability in  $\mathcal{R}_{-+}$ .

For soft-mode instabilities, we have derived an equation of motion of slow modes near the transition, which is of the form of a dynamical Cahn-Hilliard equation. The transition will generically be discontinuous (backward bifurcation) and the non-linear evolution will be characterized by regions of nucleation and of spinodal decomposition. Quenches into the supercritical regime are predicted to show coarsening behavior with a coarsening length scale growing as  $t^{1/3}$ . For hard-mode instabilities, an amplitude equation is obtained as in [2] and param-

eter regions of forward and of backward bifurcations may be distinguished by the sign of the non-linear coupling parameter.

The presented model includes and extends several previously studied models and may be considered as a minimal model for charged ion channels with internal state kinetics in a fluid membrane.

## APPENDIX A: GRADIENT EXPANSION NEAR SOFT-MODE INSTABILITIES

We transform (6-8) to the new variables

$$u = (\gamma_+ \varrho + \gamma_- \zeta) / \Gamma$$

$$v = (\varrho - \zeta) / \Gamma \quad (\text{A1})$$

and get

$$\begin{aligned} \Gamma \partial_t u = & (\gamma_+ + D\gamma_-) \nabla^2 u + \gamma_+ \gamma_- (1 - D) \nabla^2 v + \\ & + (\gamma_+ + r\gamma_-) \nabla^2 \Phi + (\gamma_+ + r\gamma_-) \nabla(u \nabla \Phi) \\ & + \gamma_+ \gamma_- \nabla(v \nabla \Phi) \end{aligned} \quad (\text{A2})$$

as equation of motion for  $u$ . Note that all terms on the *rhs* of the equation for  $u$  are at least  $O(\nabla^2)$  as a direct consequence of channel number conservation. For  $v$  we get

$$\begin{aligned} \Gamma \partial_t v = & -\Gamma^2 v + (\gamma_- + D\gamma_+) \nabla^2 v + (1 - D) \nabla^2 u + \\ & + (1 - r) \nabla^2 \Phi + (1 - r) \nabla(u \nabla \Phi) \\ & + (\gamma_- + r\gamma_+) \nabla(v \nabla \Phi) \end{aligned} \quad (\text{A3})$$

Note that  $v$  decays with a rate  $O(\nabla^0)$  due to the  $-\Gamma^2 v$  term. Thus  $v$  is fast near a soft-mode transition and may be adiabatically eliminated. It does not enter the leading order of the gradient expansion, which is obtained by replacing  $\Phi$  in (A2) from the leading ( $O(\nabla^0)$ ) order of

$$0 = (1 - \nabla^2) \Phi + \eta(u + \gamma_- v) + \alpha(u + \gamma_- v) \Phi. \quad (\text{A4})$$

This leads to

$$\partial_t u = \tau_s^{-1} \nabla^2 \left\{ \eta_c u + (1 + u) \phi(u) - \int \phi(u) du \right\} \quad (\text{A5})$$

with  $\tau_s^{-1} = (\gamma_+ + D\gamma_-) / \Gamma$  and  $\phi(u) = -\eta u / (1 + \alpha u)$ .

The linear  $O(\nabla^4)$  term is obtained from the expansion of  $\omega_+(\eta, k^2) = \tau_s^{-1} [k^2(\eta - \eta_c) / \eta_c + \xi_s^2 k^2 + O(k^4)]$ . For  $\xi_s^2$  we obtain

$$\begin{aligned} \frac{\xi_s^2}{\tau_s} = & -\frac{\eta}{2} + \frac{1}{4\Gamma} [(1 - D - \eta)^2 + 2\eta(\gamma_- - \gamma_+) - 4\eta\gamma_- Dq] \\ & - \frac{1}{4\Gamma^3} [(\gamma_- - \gamma_+)(1 - D - \eta) + 2\eta\gamma_- Dq]^2 \end{aligned} \quad (\text{A6})$$

Adding a term  $-\tau_s^{-1} \xi_s^2 \nabla^4 u$  on the *rhs* of (A5) we get (19) and (20).

## APPENDIX B: AMPLITUDE EQUATION NEAR HARD-MODE INSTABILITIES

The system of nonlinear partial differential equations (6-8) is written as  $\mathcal{L}\mathbf{u} = \mathcal{N}(\mathbf{u}, \mathbf{u})$ . In the vicinity of  $\eta_c, k_c$   $\mathbf{u} = (\varrho, \zeta, \Phi)$  contains both fast scale variations (with  $\nabla\mathbf{u} = O(k_c)$ ) and slow scale variations (with  $\nabla\mathbf{u} \rightarrow 0$  for  $\eta \rightarrow \eta_c$ ). The slowly varying part may be obtained from a perturbation expansion in  $\epsilon = \sqrt{[(\eta - \eta_c)/\eta_c]}$ , which explicitly separates slow scale variations from fast scales by introducing appropriately scaled length and time variables  $X = \epsilon x$   $T = \epsilon^2 t$ . For one-dimensional patterns, the direction perpendicular to the pattern wave vector should be scaled as  $Y = \epsilon^{1/2} y$  [18]. As functions now may depend upon fast and slow variables, we have to replace  $\partial_t \rightarrow \partial_t + \epsilon^2 \partial_T$  and  $\partial_x \rightarrow \partial_x + \epsilon \partial_X$  etc. In this way, the linear part  $\mathcal{L}$  becomes  $\mathcal{L} = \mathcal{L}_0 + \epsilon \mathcal{L}_1 + \epsilon^2 \mathcal{L}_2$ . Inserting the expansion  $\mathbf{u} = \epsilon \mathbf{u}_1 + \epsilon^2 \mathbf{u}_2 + \epsilon^3 \mathbf{u}_3 + O(\epsilon^4)$  (with  $\mathbf{u}_1(X, Y, T, x) = (\chi(X, Y, T) \exp(ik_c x) + cc)$ ) and sorting with respect to powers of  $\epsilon$  one gets a hierarchy of equations, which allows to determine  $\mathbf{u}_n$  from the  $\mathbf{u}_k$  with  $k < n$ . It starts with  $\mathcal{L}_0 \mathbf{u}_1 = 0$ , which implies that  $\mathbf{u}_1$  is an eigenstate to  $\mathcal{L}_0$  with eigenvalue zero. As  $\partial_T$  carries an explicit factor of  $\epsilon^2$ , the equation, which contains the slow time derivative of  $\mathbf{u}_1$  appears in third order in  $\epsilon$  and has the form  $\mathcal{L}_2 \mathbf{u}_1 + \mathcal{L}_1 \mathbf{u}_2 + \mathcal{L}_0 \mathbf{u}_3 = \mathcal{N}_3(\mathbf{u}_1, \mathbf{u}_2)$ . Inserting  $\mathbf{u}_2$  as obtained from the perturbation expansion in terms of  $\mathbf{u}_1$ , one gets the amplitude equation by taking the scalar product of the third order equation with the left eigenstate of  $\mathcal{L}_0$  to eigenvalue zero,  $\mathbf{u}_1^\dagger$ . This solvability condition gives

$$\int \mathbf{u}_1^\dagger \mathcal{L}_2 \mathbf{u}_1 d^2 \mathbf{r} + \int \mathbf{u}_1^\dagger \mathcal{L}_1 \mathbf{u}_2 d^2 \mathbf{r} = \int \mathbf{u}_1^\dagger \mathcal{N}_3 d^2 \mathbf{r} \quad (\text{B1})$$

The *lhs* of (B1) is linear in  $\chi$  and can be obtained directly from expanding  $\omega_+( \eta, k^2 )$  around  $\eta_c, k_c$ ,  $\omega_+( \eta, k^2 ) = \tau_h^{-1} \{ \epsilon^2 + \xi_h^2 (k - k_c)^2 + O[(k - k_c)^4] \}$ . Inserting this expansion on the *lhs* of (B1) and neglecting the  $y$  dependence for simplicity gives

$$\left( \tau_h \partial_t - \frac{\eta - \eta_c}{\eta_c} - \xi_h^2 \partial_x^2 \right) \chi = \int \mathbf{u}_1^\dagger \mathcal{N}_3 d^2 \mathbf{r} \quad (\text{B2})$$

For the time constant  $\tau_h$  we get

$$\tau_h = \frac{\Gamma + (1 + D)k_c^2 - \eta_c k_c^2 / (1 + k_c^2)}{Dk_c^2 (k_c^2 + \gamma_- + \gamma_+ / D)} \quad (\text{B3})$$

and the square  $\xi_h^2$  of the correlation length is

$$\xi_h^2 = \frac{4k_c^2}{(1 + k_c^2) (k_c^2 + \gamma_- + \frac{\gamma_+}{D})}. \quad (\text{B4})$$

Evaluating the non-linear term on the *rhs* of (B2) gives (22) with the following expression for  $J$

$$J = \frac{-\eta_c}{(k_c^2 + \gamma_- + \frac{\gamma_+}{D})(1 + k_c^2)^2} \left\{ \alpha \left( q\gamma_- + \frac{\gamma_+}{D} + k_c^2 \right) \cdot (p_1 + \Phi_{k_c} n_1 + 2\alpha) - (1 + k_c^2) \left[ 2p_1 \left( \frac{\gamma_+}{D} + k_c^2 + \zeta_{k_c} q\gamma_- \right) - \Phi_{k_c} \left\{ n_1 (\gamma_+ + k_c^2) - q\gamma_- (1 + k_c^2) z_1 \right\} \right] \right\}.$$

The expressions  $n_1, z_1$  and  $p_1$  stem from  $\mathcal{O}(\epsilon^2)$  corrections and have the form

$$n_1 = \frac{1}{18 k_c^4} \left\{ (1 + 4k_c^2)(\gamma_+ / D + 4k_c^2 + \zeta_{k_c} q\gamma_-) - 2\alpha(\gamma_+ + q\gamma_- + 4k_c^2) \right\}, \quad (\text{B5})$$

$$z_1 = \frac{n_1(\beta + 2k_c^2)(1 + 4k_c^2) + 4k_c^2(\alpha - n_1\eta_c)}{\beta(1 + 4k_c^2)(1 + k_c^2)}, \quad (\text{B6})$$

$$p_1 = \frac{(1 + k_c^2) E n_1 + \alpha}{1 + 4k_c^2}. \quad (\text{B7})$$

- 
- [1] P. Fromherz, Phys. Chem. **92** (1988) 1010
  - [2] P. Fromherz, W. Zimmermann, Phys. Rev. E **51** No. 3 (1995) 1659
  - [3] L.F. Jaffe, Nature **265** (1977) 600
  - [4] F. M. Harold, J.H. Caldwell, in *Tip Growth in Plant and Fungal Cells*, edited by I.B. Heath (Academic, New York, 1990)
  - [5] A.C. Scott, Rev. Mod. Phys. **47** (1975) 487
  - [6] E.R. Kandel, J.H. Schwartz, *Principles of Neural Science*, 2nd Ed., Elsevier, (1985)
  - [7] L.P. Savtchenko, S.M. Korogod, Neurophysiology **26** (1994) 99
  - [8] M. Léonetti and E. Dubois-Violette, Phys. Rev. E **56** (1997) 4521
  - [9] M. Léonetti and E. Dubois-Violette, Phys. Rev. Lett. **81** (1998) 1977
  - [10] M. Léonetti, Eur. Phys. J. b **2** (1998) 325
  - [11] D.J. Aidley, P.R. Stansfield, *Ion channels: molecules in action*, Cambridge University Press (1996)
  - [12] B. Hille, *Ionic Channels of Excitable Membranes*, 2nd Edition, Sinauer Associates Inc, Sunderland Massachusetts, 1992
  - [13] D.L. Nelson, M.M. Fox, in *Lehninger: Principles of biochemistry*, 3rd Ed., Worth Publishers, New York (2000)
  - [14] H.B. Peng, M. Poo, Trends Neurosci. **9** (1986) 125
  - [15] P. Fromherz, Biochim. Biophys. Acta **944** (1988) 108
  - [16] P.M. Chaikin, T.C. Lubensky, *Principles of condensed matter physics*, Cambridge, Cambridge University Press (1995)

- [17] M.C. Cross, P. Hohenberg, Rev. Mod. Phys. (1993) 851  
 [18] A.C. Newell, J.A. Whitehead, J. Fluid Mech. **38** (1969) 279

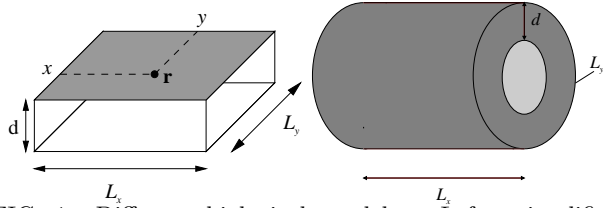


FIG. 1. Different biological models. Left: simplified synapse. Right: Model of an axon.

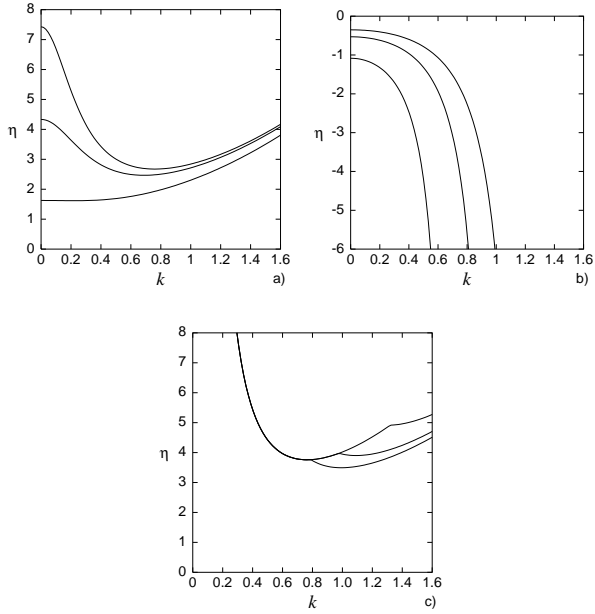


FIG. 2. Neutral curves in regions  $\mathcal{R}_{++}$  (a), and  $\mathcal{R}_{--}$  (b) for different values of  $q$ . For the upper, middle and lower curve  $q = 0.1, 0.2$  and  $0.6$  in (a),  $q = -3.0, -2.0$  and  $-1.0$  in (b) and  $q = -0.3, -0.5, -1.0$ . Other parameters are  $\gamma_+ = 0.01, \gamma_- = 0.5$  and  $D = 0.5$

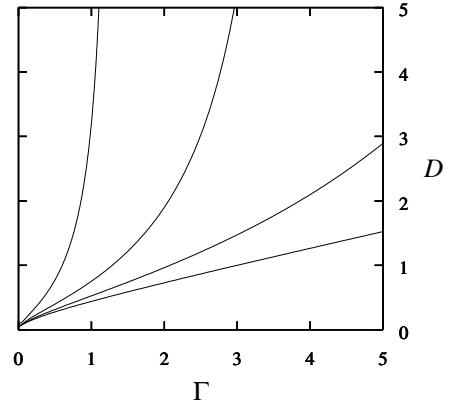


FIG. 3. Boundaries between hard-mode and soft-mode instabilities in  $D - \gamma$ -plane in  $\mathcal{R}_{++}$  for different values of  $q$ . In regions below each curve  $k_c^2 \neq 0$ . From lower to upper curves, values of  $q$  are  $0.0, 0.1, 0.25$  and  $0.5$  from lower to upper curves.

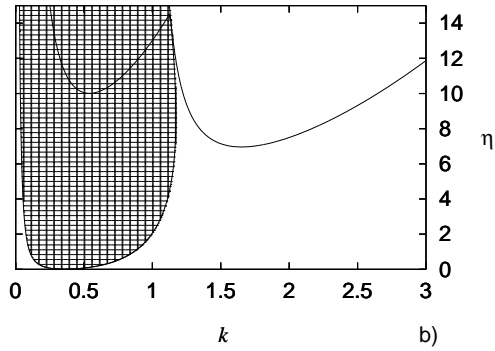
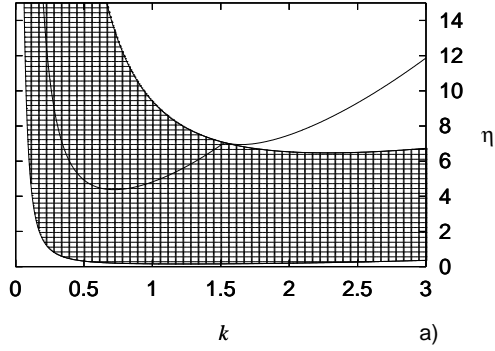


FIG. 4. Neutral curves and domain of complex eigenvalues (shaded) in  $\mathcal{R}_{-+}$  for small  $D = 0.09$  (a), and  $D = 5.0$  (b). Note that there is a discontinuous change in the nature of the transition with increasing  $D$ ; from hard-mode, stationary to hard-mode, oscillatory type. Other parameter values are  $q = -2.0$ ,  $\gamma_+ = 0.01$ ,  $\gamma_- = 0.5$ .

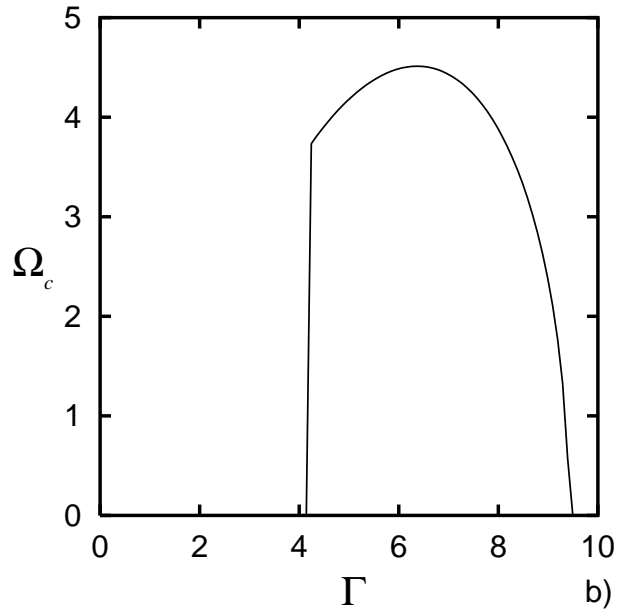
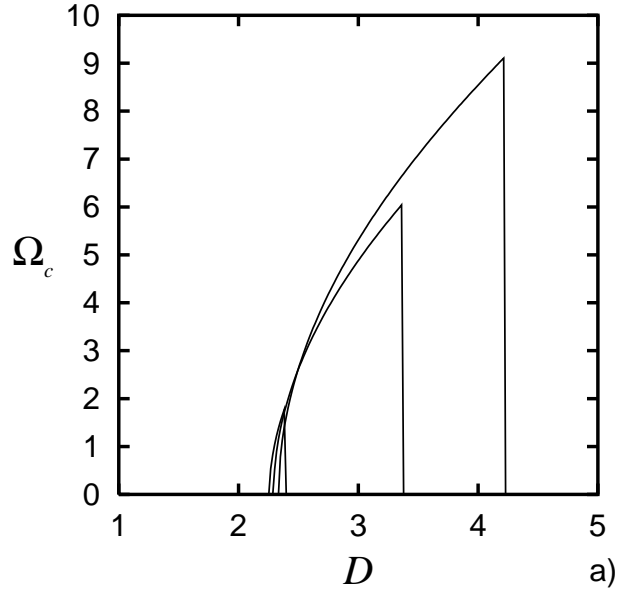


FIG. 5. The critical frequency  $\Omega_c$ : a) As function of  $D$  for  $\Gamma = 4.0, 4.5, 5.0$  and b) as a function of  $\Gamma$  for  $D = 2.75$ . The remaining parameters are  $\gamma_+ - \gamma_- = 1$  and  $q = -2$ .

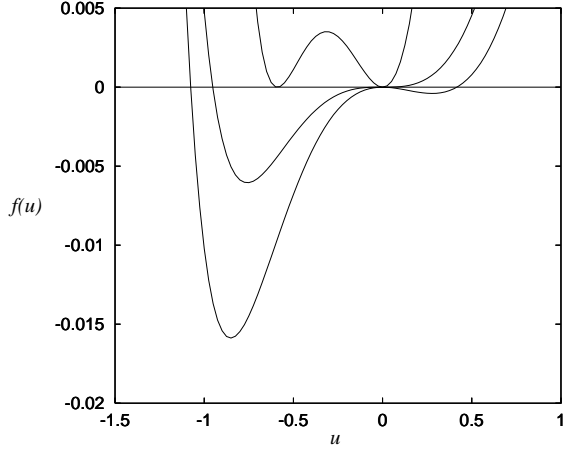


FIG. 6. Local part of the effective potential  $f(u)$ , which controls the Cahn-Hilliard dynamics near soft-mode instabilities at  $\alpha = 0.6$ . The uppermost curve displays the situation at the transition ( $\eta_c/\eta = 1.02525$ ), whereas the middle curve corresponds to the spinodal point  $\eta_c/\eta = 1$ . The lower curve is in regime at  $\eta/\eta_c = 0.97$ . For better visibility, the  $f(u)$  at the transition point has been enlarged by a factor of 10. If  $\alpha < 0.5$  the global minimum of the potential is attained for positive  $u$  and the graphs look like mirrored at the  $u = 0$ -axis.

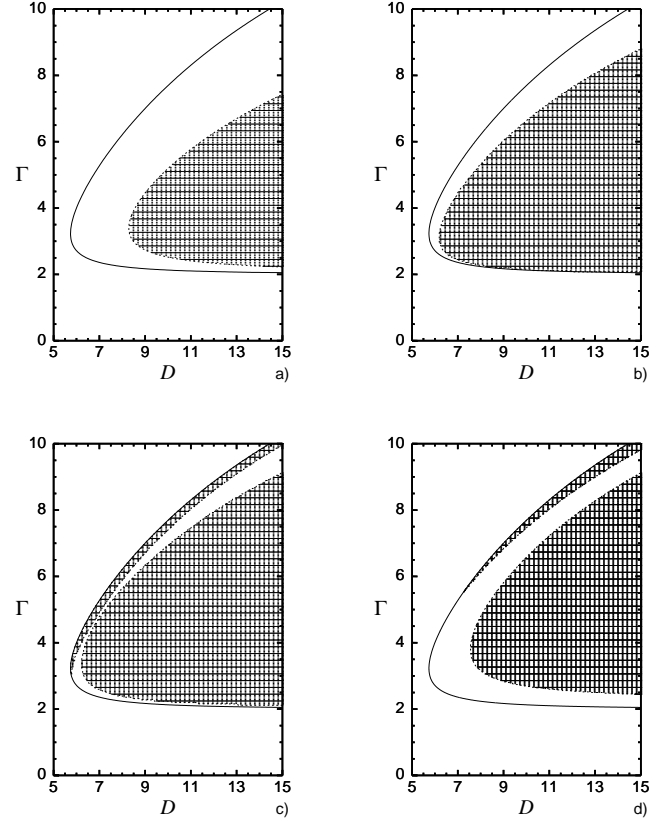


FIG. 7.  $J = 0$ -lines within the  $k_c^2 \geq 0$ -domain for  $g = 0.1$ ,  $\gamma = 2.0$  and various  $\alpha$ : (a) 0.25, (b) 0.5, (c) 0.6 and (d) 0.75. The value of  $\alpha$  crucially determines the number of domains with continuous transitions (shaded). If  $\alpha > 0.5$  the system clearly displays reentrant behavior.